Optical properties and potential applications of ε-GaSe at terahertz frequencies

Ching-Wei Chen,[1] Tsung-Ta Tang,[1] Sung-Hui Lin,[1] Jung Y. Huang,[1] Chen-Shiung Chang,[1] Pei-Kang Chung,[2] Shun-Tung Yen,[2] and Ci-Ling Pan[1,3,*]

[1]*Department of Photonics and Institute of Electro-Optical Engineering, National Chiao Tung University, Hsinchu 30010, Taiwan*
[2]*Department of Electronics Engineering, National Chiao Tung University, Hsinchu 30010, Taiwan*
[3]*Department of Physics and Institute of Photonics Technologies, National Tsing Hua University, Hsinchu 30013, Taiwan*
**Corresponding author: clpan@phys.nthu.edu.tw*

Received February 4, 2009; accepted May 4, 2009;
posted May 20, 2009 (Doc. ID 107144); published June 19, 2009

Ordinary and extraordinary refractive indices of an ε-GaSe crystal at terahertz (THz) frequencies are experimentally determined in this study. Fitting experimental data by THz time-domain spectroscopy (THz-TDS) and a Fourier transform infrared spectrometer (FTIR), we proposed revised complex dielectric functions and Sellmeier equations of GaSe for both ordinary and extraordinary waves from 0.2 to 100 THz. Phonon vibrational modes and overtones in the THz frequency range are examined in detail. The high magnitude of the figure of merit (FOM $\sim 10^3$ at 1 THz), the large birefringence ($\Delta n \sim 0.76$ at 1 THz). and the low absorption coefficient ($\alpha \sim 0.2$ cm^{-1} at 1 THz) of GaSe are also identified. Potential applications to practical photonic devices such as phase shifters at THz frequencies are proposed.

OCIS codes: 160.4330, 160.4760, 300.6300, 300.6495.

1. INTRODUCTION

Gallium selenide (GaSe) has been recognized for some time to be an important nonlinear optical crystal, particularly in the infrared range [1,2]. In recent years, GaSe has been successfully employed to generate coherent radiation in the mid-infrared and even down to the terahertz (THz) frequency range using difference frequency generation (DFG) or phase-matched optical rectification [3,4]. It has also become the material of choice for free-space electro-optical sampling of broadband THz signals [5]. As a result, a better understanding of the optical properties of a GaSe crystal is essential for optimizing nonlinear photonic devices based on this crystal. Optical constants of a GaSe crystal near the absorption edge and over a wide spectral range from the near- to the far-infrared range have been studied extensively [6–11]. The dielectric response, optical constants, and nonlinear optical properties of GaSe crystals in the THz frequency range were recently investigated by THz time-domain spectroscopy (THz-TDS) and deduced from phase matching curves of various parametric processes [12–15]. Numerous optical measurements and phonon modes of a *p*-GaSe crystal have also been reported [16]. Unfortunately, the available data on optical properties, including refractive index and absorption coefficient, of GaSe crystal in the THz region are still inconsistent.

This work reports experimental studies of a GaSe crystal's complex optical constants, including the real and imaginary parts of the ordinary dielectric function, over a wide range of THz frequencies. Fitting the experimental data, we report a revised complex ordinary and extraordinary dielectric function for a GaSe crystal. The phonon vibrational modes and overtones of GaSe in the THz frequency range are examined in detail. The high magnitude of the FOM and the large birefringence of a GaSe crystal are also identified. In view of its superior optical properties at THz frequencies, we also propose the design of a GaSe based THz phase modulator.

2. EXPERIMENTAL METHODS

The GaSe crystals investigated in this work were grown using the Bridgman method. Raw materials were placed in a clean quartz tube, sealed, and then pumped down to below 10^{-6} Torr. Crystals were grown at a thermal gradient of 30°C/cm with a growth rate of 2 cm/day. The resulting pure GaSe crystal exhibited the characteristic appearance of a (001) hexagonal layered structure. The optical transmission of a thin GaSe crystal of a thickness of ~170 μm was determined using a Bruker IFS66v/S spectrometer (Fourier transform infrared spectrometer—FTIR) over a wide range of frequencies (60–4000 cm^{-1}). The power reflectivity from a thick GaSe crystal (thickness ~3 mm) surface was also measured by the specular reflection method with an oblique angle of incidence ($\theta \sim 11°$) using the FTIR. Three GaSe crystals with thicknesses of 287 μm, 1110 μm, and 2021 μm were prepared for the THz-TDS measurement. A homemade antenna-based THz-TDS system with a collimated beam at the sample position was used [17]. Briefly, THz pulses generated from a femtosecond laser-excited dipole-type antenna fabricated on low-temperature-grown GaAs were collimated by an off-axis paraboloidal mirror and propagated through the GaSe sample at normal incidence. The

transmitted THz pulses were focused on another dipole-type antenna that was gated by time-delayed probe pulses and oriented to detect THz waves that were polarized parallel to the incident THz wave polarization. The diameter of the beam of the THz wave through the GaSe sample was approximately 0.6 cm. The THz spectrometer was purged with nitrogen and maintained at a relative humidity of 3.0±0.5%.

3. RESULTS AND DISCUSSIONS

A. Extraction of Complex Optical Constants from THz-TDS Measurement

A THz pulse propagating through the reference or the sample is referred to as a reference pulse or sample pulse, characterized by their measured electric fields $E_r(t)$ and $E_s(t)$, respectively. The complex refractive index of the sample is represented by the refractive index n_s and the extinction coefficient k_s. These were calculated at each frequency f from the ratio of the Fourier transforms of the time-domain THz waveforms of the sample pulse and the reference pulse $E_s(f)$ and $E_r(f)$, i.e.,

$$\sqrt{T}e^{i\varphi} = \frac{E_s(f)}{E_r(f)} = \left[\tilde{t}_{AS}\tilde{t}_{SA}\sum_{m=0}^{N}[\tilde{r}_{SA}e^{i2\pi f(\tilde{n}_S d_S/c)}]^{2m}e^{-2\pi f/c[(k_S-k_A)d_S]}\right] \times e^{i2\pi f/c[(n_S-n_A)d_S]}. \quad (1)$$

T and φ are the power transmittance and the phase shift for sample and reference pulses, respectively; d_s is the thickness of sample; and $\tilde{n}_S$ and $\tilde{n}_A$ are the complex refractive indices of sample and air, respectively. $\tilde{t}_{AS}=2\times\tilde{n}_A/(\tilde{n}_A+\tilde{n}_S)$ and $\tilde{t}_{SA}=2\times\tilde{n}_S/(\tilde{n}_S+\tilde{n}_A)$ are the Fresnel transmission coefficients at the air–sample and sample–air interfaces, respectively. $\tilde{r}_{SA}=(\tilde{n}_S-\tilde{n}_A)/(\tilde{n}_S+\tilde{n}_A)$ is the Fresnel reflection coefficient at the sample–air interface. From Eq. (1), the complex refractive index $\tilde{n}_S=n_S+ik_S$ is derived as follows:

$$n_S = \frac{1}{2\pi f\frac{d_S}{c}}\left[\varphi - \arg\left(\tilde{t}_{AS}\tilde{t}_{SA}\sum_{m=0}^{N}[\tilde{r}_{SA}e^{i2\pi f(\tilde{n}_S d_S/c)}]^{2m}e^{-2\pi f/c[(k_S-k_A)d_S]}\right)\right] + n_A\ , \quad (2)$$

$$k_S = \frac{1}{-2\pi f\frac{d_S}{c}}\ln\left[\frac{\sqrt{T}}{|\tilde{t}_{AS}\tilde{t}_{SA}\Sigma_{m=0}^{N}[\tilde{r}_{SA}e^{i2\pi f(\tilde{n}_S d_S/c)}]^{2m}e^{-2\pi f/c[(k_S-k_A)d_S]}|}\right] + k_A. \quad (3)$$

GaSe crystals of different sample thicknesses (d =287, 1110, 2021 μm) were investigated. The extracted values of the real part of the complex ordinary refractive indices for the three crystals are mutually consistent. Figure 1(a) depicts the temporal THz waveforms transmitted through air and the GaSe crystal with a thickness d =1110 μm. The relatively clean separation in the time domain of the main transmitted pulse and that due to the first internal reflection facilitated the data analysis for the optical constants. Following an iterative calculation procedure, we determined that the real part of the complex ordinary refractive index n_o, presented in Fig. 1(b), is about 3.23–3.37 (±0.005) in the range from 0.2 THz to 3 THz.

The complex refractive index $\tilde{n}$ of a dispersive medium depends on frequency. In regions of the spectrum where the material does not absorb, the real part of the complex refractive index tends to increase with frequency. Near the anomalous dispersion and resonant absorption, the refractive index can decrease with frequency [18]. The imaginary indices of the refraction of GaSe, which is shown in Fig. 1(c), clearly indicates the presence of an absorption peak at around 0.586 THz (19.5 cm^{-1}), which is responsible for the observed ringing in the time-domain waveform in Fig. 1(a). The presence of the resonance peak of the "rigid layer mode" at 0.586 THz indicates that the pure GaSe crystal is in the ε phase. As expected, the real part of the refraction index for ordinary wave n_o exhibits dispersive behavior close to the absorption peak [see Fig. 1(b)]. Figure 1(c) shows that the extinction coefficient for ordinary wave k_o to be in the range of 0.0013–0.0188, sufficiently removed from the absorption peak. This value corresponds to an absorption coefficient of under 20 cm^{-1} in the 0.2–3 THz frequency range.

B. FTIR Transmission-Type Measurement

Fourier-transform infrared transmission spectra are useful for characterizing phonon vibration frequencies. Earlier we identified some overtones and multiphonon process modes of GaSe [10,11]. Figure 2 depicts the experimental absorption spectrum of a pure GaSe crystal in a wide wavelength range from the near- to the far-infrared range (3–700 μm). We note that data obtained by two different measuring techniques (FTIR and THz-TDS), shown as the different symbols in Fig. 2, are combined to generate this broadband absorption spectrum. Some other IR active modes at 19.6 μm (510 cm^{-1}), 22.4 μm (446 cm^{-1}), 24.4 μm (410 cm^{-1}), and 27.6 μm (362 cm^{-1}) are identified. These modes are assigned to the difference frequency combinations of acoustic and optical

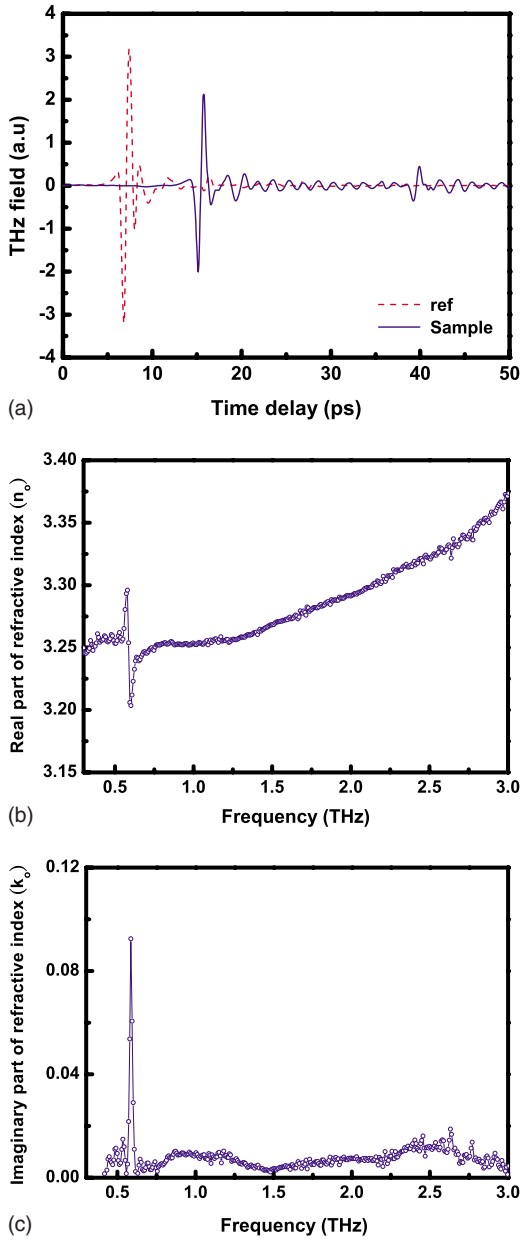

Fig. 1. (Color online) (a) Waveforms of the THz pulse transmitted through GaSe crystal of thickness $d = 1.110$ mm (solid curve) and the reference pulse (dashed curve). (b) Real part of the complex refractive index of the GaSe crystal for ordinary wave n_o. (c) Imaginary part of the complex refractive index of the GaSe crystal for ordinary wave k_o.

phonons or impurity-induced localized modes. For instance, the band at 24.4 μm is the overtone of the IR active mode at 46.8 μm. The band at 27.6 μm originates from the multiphonon processes, while the two bands at 19.6 μm and 22.4 μm are attributed mainly to the impurity-induced localized modes [12,16,19,20].

In principle, the optical medium indeed absorbs very strongly whenever the photon is close to resonance with the transverse optical (TO) phonon. The fundamental optical properties of a dielectric, including the absorption, refraction and reflectivity, are all related to each other because they are all determined by the complex dielectric function. At frequencies in the reststrahlen band between

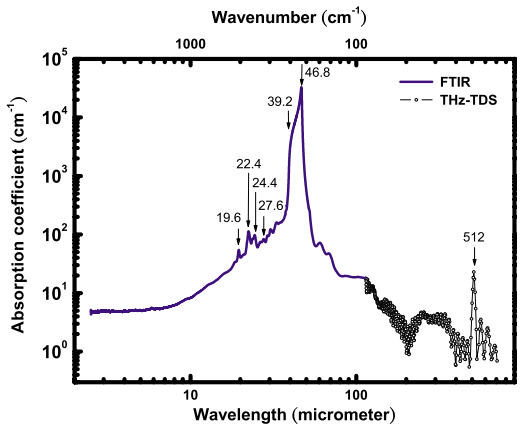

Fig. 2. (Color online) Absorption spectrum of pure GaSe crystal from 3 μm to 700 μm. Data from FTIR and THz-TDS are combined.

TO and longitudinal optical (LO) phonons, no mode can propagate and so all of the incident photons are reflected. For example, Yamamoto *et al.* determined the complex refractive index through the Kramers–Kronig analysis of the reflection spectrum from a single interface of the dielectric [21]. Accordingly, the strong infrared absorption peak in the reststrahlen band, which provides the information about the phonon modes and absorption coefficient, are determined by measuring the crystal surface reflectivity, to be mentioned later. The results are depicted in Fig. 2 in the wavelength range 30–50 μm.

C. FTIR Reflection-Type Measurement

Figure 3 shows spectral power reflectance of a GaSe crystal, which yields information about optical phonons in the reststrahlen band. The data in the frequency range of 3–15 THz were experimentally measured by the FTIR. The spectral power reflectance in the range from 0.2 to 3 THz, R(ω) for an incidence angle of $\theta_0 \sim 11°$, were

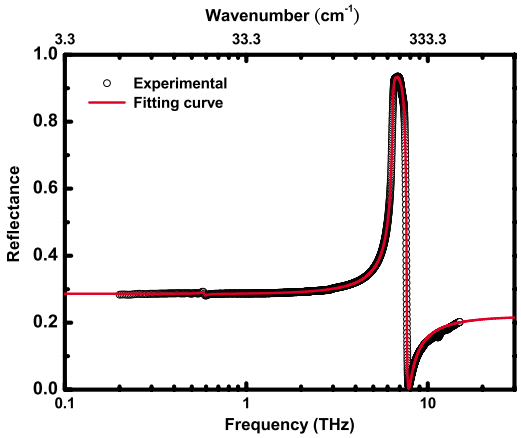

Fig. 3. (Color online) Power reflectance of GaSe from 0.2 to 15 THz. A strong infrared absorption peak in the range 6–8 THz, the reststrahlen band, is identified. The open circles are experimentally measured values. The solid curve is the best-fit curve.

calculated by using the complex refractive indices of the GaSe crystal from the THz-TDS experiments as follows:

$$R(\omega) = \left[\frac{n_A \cos\theta_0 - \sqrt{(n_s(\omega) + ik_s(\omega))^2 - (n_A \sin\theta_0)^2}}{n_A \cos\theta_0 + \sqrt{(n_s(\omega) + ik_s(\omega))^2 - (n_A \sin\theta_0)^2}} \right]^2 , \quad (4)$$

where $n_A = 1$ corresponds to the refractive index of air; and $n_s(\omega)$ and $k_s(\omega)$ represent the refractive index and extinction coefficients of the GaSe sample, respectively, at any angular frequency ω. Combining the results from THz-TDS and reflectance FTIR, we obtained the power reflectance over a wide frequency range from 0.2 to 15 THz, as shown in Fig. 3.

D. Complex Dielectric Function and the Sellmeier Equations

Starting from the parameters and formulism given in [1], we have developed theoretically the complex dielectric function for ordinary waves to fit our spectral reflectance data. This is presented as the solid curve in Fig. 3. The complex dielectric function for ordinary wave $\varepsilon_o(\omega)$ is written as

$$\varepsilon_o(\omega) = A\omega^6 + B\omega^4 + C\omega^2 + S_1 + \frac{(\omega_L^2 - \omega_T^2)S_1}{\omega_T^2 - \omega^2 - i\Gamma_1\omega} + \frac{\omega_t^2 S_2}{\omega_t^2 - \omega^2 - i\Gamma_2\omega} , \quad (5)$$

where ω is in wave numbers, $A = 6.105 \times 10^{-27}$ cm^6, $B = 1.8564 \times 10^{-18}$ cm^4, $C = 4.0499 \times 10^{-9}$ cm^2, $S_1 = 7.37$, $S_2 = 0.017$, $\Gamma_1 = 2.8$ cm^{-1}, $\Gamma_2 = 0.5667$ cm^{-1}, $\omega_L = 255$ cm^{-1}, $\omega_T = 213.5$ cm^{-1}, and $\omega_t = 19.53$ cm^{-1}. Note that we have introduced damped harmonic oscillator terms for phonons. Although the coefficients of A, B, and C are small, we still include these in order to deduce the Sellmeier equations for a GaSe crystal to be described later. After the experimental data were fitted, the transverse and longitudinal optical phonons (ω_{TO} and ω_{LO}) are identified at 46.8 μm (6.40 THz, 213.5 cm^{-1}) (E′(TO)), and 39.2 μm (7.65 THz, and 255 cm^{-1}) (E′(LO)), respectively. Both assigned phonon modes in the reststrahlen band in our studies are consistent with those reported elsewhere [1,10]. The infrared active phonons identified this way also confirm that the GaSe crystal investigated in this work is in the ε phase.

For comparison, we have plotted ordinary refractive indices and absorption coefficients of GaSe crystals reported in previous works together with our results in Fig. 4. The optical constants measured herein agree closely with the data published by Singh *et al.* [14]. The sharp phonon resonance mode we measured at 0.586 THz is also verified in that work [14]. Other studies have also obtained optical constants using THz-TDS in the THz range [12,13]. However, the optical constants in these studies deviate somewhat from those measured in this investigation. In particular, we did not observe any second-order phonon vibration mode as reported by Yu *et al.* [12]. It can be seen that the proposed dielectric function for ordinary waves fits our experimental data for the refractive index and absorption coefficient in the THz range very well (see Fig. 4).

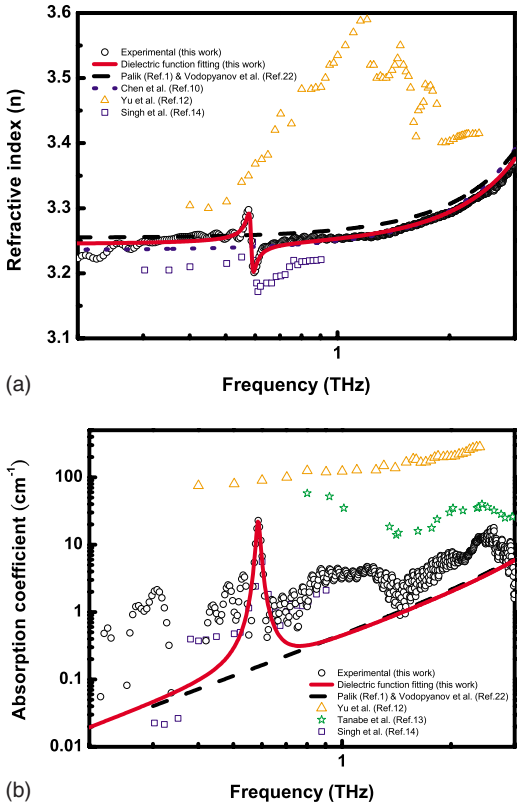

Fig. 4. (Color online) (a) Comparisons of ordinary refractive indices n_o of GaSe herein and published values. Fitting curve is obtained by fitting with the dielectric function in this work. (b) Comparison of ordinary absorption coefficient α of GaSe herein and published values. Fitting curve is obtained by fitting with the dielectric function in this work.

The Sellmeier equation is an empirical formula that effectively describes dispersion. Previously, several groups have proposed the Sellmeier equation for a pure GaSe crystal suitable over various frequency ranges [10,22,23]. In particular, Shi *et al.* utilized the dispersion relation of Vodopyanov *et al.* [24] to confirm the phase-matching condition for generation of coherent THz radiation by difference frequency mixing. In our previous investigation [10], we reported revised Sellmeier equations that were expected to be accurate over the spectral range of 2.4–35 μm. These were found to fit the experimentally measured phase-matching curve from 2.4 to 28 μm. In Figs. 4(a) and 4(b), the different symbols represent the refractive indices and absorption coefficients for ordinary waves n_o and α_o calculated using dielectric functions reported in the literature [1,10,22].

Because of the orientation of the crystal available to us, we were unable to measure the optical constant of GaSe for extraordinary waves in the THz frequency range and establish an expression for the corresponding dielectric function. Alternatively, we first fit the experimental data for phase matching of mid-infrared difference frequency mixing in our previous work [10] and the dielectric function for ordinary waves [Eq. (5)]. This is illustrated in Fig. 5(a). The best-fit complex dielectric function for extraordinary wave is found to be:

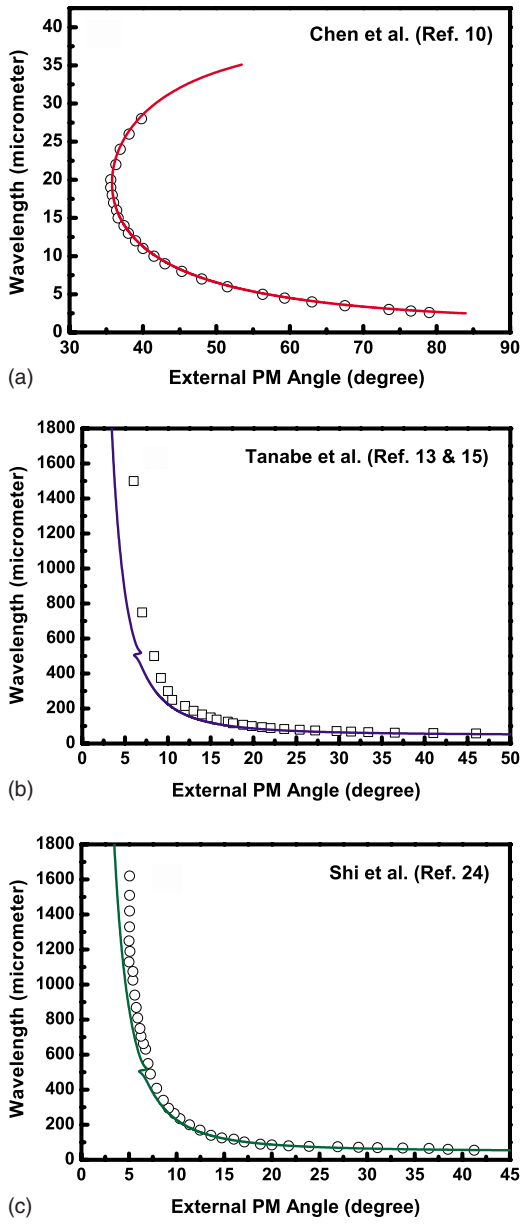

Fig. 5. (Color online) (a) Fitting of the phase-matching curve for difference frequency generation (DFG) in the infrared range [10] to obtain the extraordinary refractive index n_e of GaSe. (b) Fitting of the phase-matching curve for generation of THz radiation by DFG in [13,15]. (c) Fitting of the phase matching curve for generation of THz radiation by DFG in [24].

$$\varepsilon_e(\omega) = A'\omega^6 + B'\omega^4 + C'\omega^2 + S_3 + \frac{(\omega_L^2 - \omega_T^2)S_3}{\omega_T^2 - \omega^2 - i\Gamma_3\omega} \quad , \quad (6)$$

where $A' = 122.3 \times 10^{-27}$ cm^6, $B' = -22.88 \times 10^{-18}$ cm^4, $C' = 3.879 \times 10^{-9}$ cm^2, $S_3 = 5.76$, $\Gamma_3 = 2.8$ cm^{-1}, $\omega_L = 245.5$ cm^{-1}, and $\omega_T = 237$ cm^{-1}. Equation (6) is reliable in the THz regime as well. This is verified by fitting the phase-matching curves for coherent generation of THz generation reported in the literature. These are shown in Figs. 5(b) and 5(c) [13,15,24]. It can be seen that the dielectric functions reported in this work are in good agreement with experimental data except for some deviations in the long wavelength ranges. Possibly this resulted from the bandwidth of the two interacting waves in the difference frequency mixing process.

Employing the revised dielectric functions in Eqs. (5) and (6), we propose the following modified Sellmeier equations for GaSe suitable for a wide range of frequencies. For o-ray,

$$n_o^2 = A + \frac{B}{\lambda^2} + \frac{C}{\lambda^4} + \frac{D}{\lambda^6} + \frac{E\lambda^2}{\lambda^2 - F} + \frac{G\lambda^2}{\lambda^2 - H} \quad , \quad (7)$$

where λ is the wavelength in micrometers, and A=7.37, B=0.405, C=0.0186, D=0.0061, E=3.1436, F=2193.8, G=0.017, and H=262177.5577. The last term is added to take into account the phonon modes ($\omega_t = 19.53$ cm^{-1}) observed in the THz range. Similarly, the modified Sellmeier equation for e-ray is given by

$$n_e^2 = A' + \frac{B'}{\lambda^2} + \frac{C'}{\lambda^4} + \frac{D'}{\lambda^6} + \frac{E'\lambda^2}{\lambda^2 - F'} \quad , \quad (8)$$

with A′=5.76, B′=0.3879, C′=−0.2288, D′=0.1223, E′=0.4206, and F′=1780.3. Figure 6(a) presents the extraordinary refractive indices of GaSe from 0.2 to 3 THz deduced in this work according to Eqs. (6) and (8) and the Sellmeier equation reported by other groups [1,22], including that of our previous work [10]. Figure 6(b) shows the extraordinary refractive index of GaSe in a wide range of frequencies from 0.2 to 100 THz, highlighting

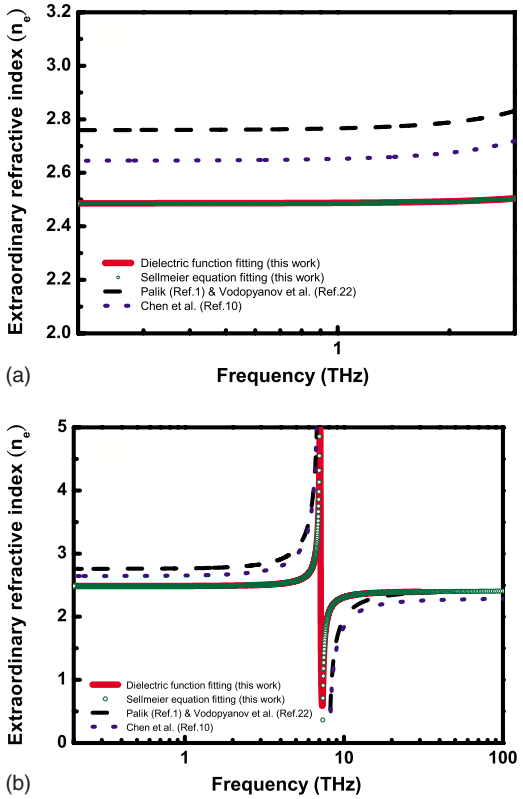

Fig. 6. (Color online) (a) Comparisons of extraordinary refractive indices n_e of GaSe herein and published values. The solid curves are obtained by fitting with the dielectric function and Sellmeier equations in this work. (b) The extraordinary refractive index of GaSe from 0.2 to 100 THz. The meanings of the symbols are the same as in Fig. 6(a). Resonance due to the transverse phonon is clearly represented.

Table 1. Parameters Used in the Calculation of the Dielectric Functions for ε-GaSe in Eqs. (5) and (6) with Corresponding Values from the Handbook [1] for Comparison

Ordinary			Extraordinary		
Parameter	*This work*	*Ref. [1]*	*Parameter*	*This work*	*Ref. [1]*
A (cm^6)	6.105×10^{-27}	6.105×10^{-27}	A′ (cm^6)	122.3×10^{-27}	
B (cm^4)	1.8564×10^{-18}	1.8564×10^{-18}	B′ (cm^4)	-22.88×10^{-18}	
C (cm^2)	4.0499×10^{-9}	4.0499×10^{-9}	C′ (cm^2)	3.879×10^{-9}	
S_1	7.37	7.443	S_3	5.76	5.76
S_2	0.017				
Γ_1 (cm^{-1})	2.8	3	Γ_3 (cm^{-1})	2.8	2.8
Γ_2 (cm^{-1})	0.5667				
ω_L (cm^{-1})	255	254.7	ω_L (cm^{-1})	245.5	245.5
ω_T (cm^{-1})	213.5	213.5	ω_T (cm^{-1})	237	237
ω_t (cm^{-1})	19.53				

Table 2. Parameters Used in the Calculation of the Sellmeier Equations for ε-GaSe in Eqs. (7) and (8) with Corresponding Values from [22] for Comparison

Ordinary (n_o)			Extraordinary (n_e)		
Parameter	*This work*	*Ref. [22]*	*Parameter*	*This work*	*Ref. [22]*
A	7.37	7.443	A′	5.76	5.76
B	0.405	0.405	B′	0.3879	0.3879
C	0.0186	0.0186	C′	−0.2288	−0.2288
D	0.0061	0.0061	D′	0.1223	0.1223
E	3.1436	3.1485	E′	0.4206	1.855
F	2193.8	2194	F′	1780.3	1780
G	0.017				
H	262177.5577				

the dispersion near the strong resonance due to the transverse optical phonon.

The coefficients for the dielectric function of GaSe as given in Eqs. (5) and (6) are listed in Table 1. The corresponding indices listed in the handbook [1] are also summarized in Table 1 for comparison. Similarly, coefficients for the Sellmeier equations of GaSe in Eqs. (7) and (8) as well as those published in [22] are summed up in Table 2.

E. Potential Applications

The GaSe crystal is a promising material for nonlinear optical and optoelectronic applications at THz frequencies. The nonlinear optical coefficient of a GaSe crystal is $d_{22}=54$ pm/V [2]. The highest electro-optic coefficient of a GaSe crystal is $r_{22}=14.4$ pm/V, more than three times higher than $r_{41}=4$ pm/V of the ZnTe crystal [25]. In Fig. 7(a) we have plotted the FOM of the GaSe crystal, defined as $d_{eff}^2/n^3\alpha^2$, as a function of frequency. The FOM of GaSe is as high as 10^3 at 1 THz. For comparison, we have also calculated the FOM of $LiNbO_3$ at THz frequencies [26], which is approximately five orders of magnitude larger than that for bulk $LiNbO_3$. Hence, the GaSe crystal is expected to be a good candidate for generating and frequency mixing of THz waves. Not only does it have a low absorption coefficient ($\sim$2 cm^{-1} at 1 THz) at THz frequencies, it also has a large birefringence $\sim$0.76 at 1 THz, as shown in Fig. 7(b). The birefringence of GaSe presented in this study is calculated from our revised ordinary and extraordinary dielectric functions. The high birefringence and low absorption coefficient of GaSe renders the crystal attractive for THz device applications. For example, a GaSe crystal thickness of 400 μm would be required for achieving a 2π phase shift at 1 THz ($\lambda=300$ μm). The low intrinsic absorption loss in the GaSe crystal is such that transmittance could be as high as 92% for a crystal with a thickness of 400 μm. We have previously reported liquid-crystal-based THz phase shifters [27,28]. The birefringence of typical nematic liquid crystals is of the order of 0.2 or less [29,30]. As a result, a thickness of several millimeters is required for the liquid crystal. Other practical applications of the design of photonic devices at THz frequencies are anticipated.

4. CONCLUSIONS

The optical constants of ε-GaSe over the THz frequency range are determined in this study. In the band of 0.2 to 3 THz, the ordinary refractive index n_o is 3.23–3.37 ($\pm$0.005), while the ordinary extinction coefficient k_o is in the range of 0.0013–0.0188. A low-frequency rigid-layer phonon mode observed at 0.586 THz further confirms the pure GaSe crystal to be in the ε phase. We also identified transverse and longitudinal optical phonons in the reststrahlen band at 6.39 and 7.62 THz, respectively, by ana-

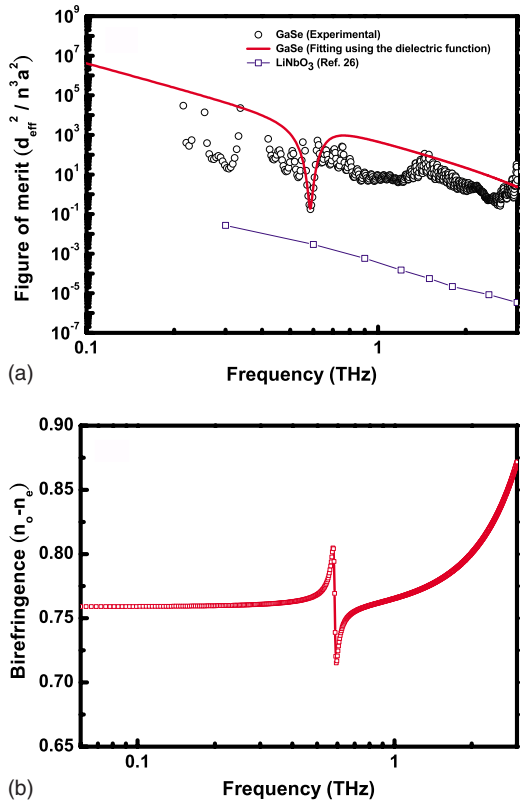

Fig. 7. (Color online) (a) Comparison of FOM of GaSe and $LiNbO_3$ crystals in the THz frequency range. Open circles are FOM of GaSe using the experimental data of this work. Solid curve is fitting of the experimental data by the dielectric function. Open squares are values of FOM for $LiNbO_3$. (b) Birefringence of GaSe crystal at terahertz frequencies.

lyzing results of the FTIR measurements. The revised dielectric functions and Sellmeier equations for both ordinary and extraordinary waves are reported. These are shown to be accurate over a broad range of frequencies from 0.2 to 100 THz. The FOM for GaSe crystal is as high as 10^3 at 1 THz. It also exhibits high birefringence ($\sim$0.76 at 1 THz) and a low absorption coefficient ($\sim$2 cm^{-1} at 1 THz). ε-GaSe crystal is thus a good candidate for photonic devices such as phase shifters at THz frequencies.

ACKNOWLEDGMENTS

The authors thank the National Science Council of Taiwan (NSCT) for financially supporting this research under contracts NSC-95-2221-E-009-123 and NSC-96-2120-M-009-007 and the Program for the Pursuit of Academic Excellence in Universities, Phase II (PPAEU-II). The authors are also sponsored by National Nano Device Laboratory and the Academic Top Universities (ATU) Program of the Ministry of Education, Taiwan.

REFERENCES

1. E. D. Palik, *Handbook of Optical Constants of Solids* (Academic, 1998), Vol. III.
2. V. G. Dmitriev, G. G. Gurzadyan, and D. N. Nikogosyan, *Handbook of Nonlinear Optical Crystals* (Springer, 1997), pp. 166–169.
3. W. Shi and Y. J. Ding, "A monochromatic and high-power terahertz source tunable in the ranges of 2.7–38.4 and 58.2–3540 μm for variety of potential applications," Appl. Phys. Lett. **84**, 1635–1637 (2004).
4. R. Huber, A. Brodschelm, F. Tauser, and A. Leitenstorfer, "Generation and field-resolved detection of femtosecond electromagnetic pulses tunable up to 41 THz," Appl. Phys. Lett. **76**, 3191–3193 (2000).
5. K. Liu, J. Xu, and X. C. Zhang, "GaSe crystals for broadband terahertz wave detection," Appl. Phys. Lett. **85**, 863–865 (2004).
6. S. Adachi and Y. Shindo, "Optical constants of ε-GaSe," J. Appl. Phys. **71**, 428–431 (1992).
7. N. Piccioli, R. Le Toullec, M. Mejatty, and M. Balkanski, "Refractive index of GaSe between 0.45 μm and 330 μm," Appl. Opt. **16**, 1236–1238 (1976).
8. V. M. Burlakov, E. A. Vinogradov, G. N. Zhizhin, N. N. Mel'nik, D. A. Rzaev, and V. A. Yakovlev, "Optical properties of GaSe films at lattice vibration frequencies," Sov. Phys. Solid State **21**, 1477–1480 (1979).
9. K. Allakhverdiev, N. Fernelius, F. Gashimzade, J. Goldstein, E. Salaev, and Z. Salaeva, "Anisotropy of optical absorption in GaSe studied by midinfrared spectroscopy," J. Appl. Phys. **93**, 3336–3339 (2003).
10. C. W. Chen, Y. K. Hsu, J. Y. Huang, C. S. Chang, J. Y. Zhang, and C. L. Pan, "Generation properties of coherent infrared radiation in the optical absorption region of GaSe crystal," Opt. Express **14**, 10636–10644 (2006).
11. Y. K. Hsu, C. W. Chen, J. Y. Huang, C. L. Pan, J. Y. Zhang, and C. S. Chang, "Erbium doped GaSe crystal for mid-IR applications," Opt. Express **14**, 5484–5491 (2006).
12. B. L. Yu, F. Zeng, V. Kartazayev, R. R. Alfano, and K. C. Mandal, "Terahertz studies of the dielectric response and second-order phonons in a GaSe crystal," Appl. Phys. Lett. **87**, 182104 (2005).
13. T. Tanabe, K. Suto, J.-I. Nishizawa, and T. Sasaki, "Characteristics of terahertz-wave generation from GaSe crystals," J. Phys. D **37**, 155–158 (2004).
14. N. B. Singh, T. B. Norris, T. Buma, R. N. Singh, M. Gottlieb, D. Suhre, and J. J. Hawkins, "Properties of nonlinear optical crystals in the terahertz wavelength region," Opt. Eng. (Bellingham) **45**, 094002 (2006).
15. J.-I. Nishizawa, T. Sasaki, Y. Oyama, and T. Tanabe, "Aspects of point defects in coherent terahertz-wave spectroscopy," Physica B **401–402**, 677–681 (2007).
16. K. Allakhverdiev, T. Baykara, S. Ellialtioglu, F. Hashimzade, D. Huseinova, K. Kawamura, A. A. Kaya, A. M. Kulibekov (Gulubayov), and S. Onari, "Lattice vibrations of pure and doped GaSe," Mater. Res. Bull. **41**, 751–763 (2006).
17. C. L. Pan, C. F. Hsieh, R. P. Pan, M. Tanaka, F. Miyamaru, M. Tani, and M. Hangyo, "Control of enhanced THz transmission through metallic hole arrays using nematic liquid crystal," Opt. Express **13**, 3921–3930 (2005).
18. B. E. A. Saleh and M. C. Teich, *Fundamentals of Photonics* (Wiley, 1991).
19. H. Yoshida, S. Nakashima, and A. Mitsuishi, "Phonon Raman spectra of layer compound GaSe," Phys. Status Solidi B **59**, 655–666 (1973).
20. M. Hayek, O. Brafman, and R. M. A. Lieth, "Splitting and coupling of lattice modes in the layer compounds GaSe, GaS, and $GaSe_xS_{1-x}$," Phys. Rev. B **8**, 2772–2779 (1973).
21. K. Yamamoto, A. Masui, and H. Ishida, "Kramers-Kronig analysis of infrared reflection spectra with perpendicular polarization," Appl. Opt. **33**, 6285–6293 (1994).
22. K. L. Vodopyanov and L. A. Kulevskii, "New dispersion relationships for GaSe in the 0.65–18 μm spectral region," Opt. Commun. **118**, 375–378 (1995).
23. K. R. Allakhverdiev, T. Baykara, A. K. Gulubayov, A. A. Kaya, J. Goldstein, N. Fernelius, S. Hanna, and Z. Salaeva, "Corrected infrared Sellmeier coefficients for gallium selenide," J. Appl. Phys. **98**, 093515 (2005).
24. W. Shi, Y. J. Ding, N. Fernelius, and K. Vodopyanov, "Efficient, tunable, and coherent 0.18–5.27-THz source based on GaSe crystal," Opt. Lett. **27**, 1454–1456 (2002).
25. C. Kubler, R. Huber, and A. Leitenstorfer, "Ultrabroadband

terahertz pulses: generation and field-resolved detection," Semicond. Sci. Technol. **20**, S128–S133 (2005).
26. Y. J. Ding and W. Shi, "Widely-tunable, monochromatic, and high-power terahertz sources and their applications," J. Nonlinear Opt. Phys. Mater. **12**, 557–585 (2003).
27. C. Y. Chen, C. F. Hsieh, Y. F. Lin, R. P. Pan, and C. L. Pan, "Magnetically tunable room-temperature 2π liquid crystal terahertz phase shifter," Opt. Express **12**, 2625–2630 (2004).
28. H. Y. Wu, C. F. Hsieh, T. T. Tang, R. P. Pan, and C. L. Pan, "Electrically tunable room-temperature 2π liquid crystal terahertz phase shifter," IEEE Photonics Technol. Lett. **18**, 1488–1490 (2006).
29. T. R. Tsai, C. Y. Chen, C. L. Pan, R. P. Pan, and X. C. Zhang, "THz time-domain spectroscopy studies of the optical constants of the nematic liquid crystal 5CB," Appl. Opt. **42**, 2372–2376 (2003).
30. R. P. Pan, C. F. Hsieh, C. L. Pan, and C. Y. Chen, "Temperature-dependent optical constants and birefringence of nematic liquid crystal 5CB in the terahertz frequency range," J. Appl. Phys. **103**, 093523 (2008).